DEPARTMENT OF THE INTERIOR

U.S. GEOLOGICAL SURVEY

FOUR CONTRIBUTIONS TO:

2ND SEMINAR ON LANDSLIDE HAZARDS

COSENZA, ITALY; MARCH 5-6, 1990

BY

WIECZOREK, G.F.[1], SCHUSTER, R.L.[2], HARP, E.L.[3],

FLEMING, R.W.[2], BAUM, R.L.[2], AND JOHNSON, A.M.[4]

Open-File Report 91-108

[1]USGS, Reston, VA 22092, [2]USGS, Denver, CO 80225,[3]USGS, Menlo Park, CA 94025, [4]Purdue University, West Lafayette, Indiana 47907

Reston, Virginia

March 1, 1991

FOUR CONTRIBUTIONS TO:
2ND SEMINAR ON LANDSLIDE HAZARDS
COSENZA, ITALY; MARCH 5-6, 1990

TABLE OF CONTENTS

DIRECTIONS OF THE USGS LANDSLIDE HAZARDS REDUCTION PROGRAM

by

Gerald F. Wieczorek

INTRODUCTION

In the United States, studies of landslides are conducted by scientists and engineers of government agencies, universities, and private consulting companies. In 1980 the United States Congress authorized the U.S. Geological Survey (USGS) Landslide Hazards Reduction Program; in fiscal year 1990, the program was funded at a level of approximately $2.2 million. The USGS's Landslide Hazards Reduction Program is a focal point of landslide research in the United States Government. Landslide research within the USGS is conducted by a professional staff of 15 geologists and engineers from offices in Reston, Virginia; Denver, Colorado; and Menlo Park, California. Scientists with State governments have been contracted or have entered into cooperative arrangements with the USGS to carry out additional landslide investigations. The main components of the program include studies of landslide process and prediction, landslide susceptibility and risk mapping, landslide recurrence and slope evolution, and research applications and technology transfer. This paper describes the highlights of recent accomplishments, descriptions of work underway, and directions of future research. Locations of landslide studies described in this paper are shown in Figure 1.

PROCESS AND PREDICTION

In October of 1985 tropical storm Juan struck southern Puerto Rico and triggered hundreds of landslides (Jibson, 1989). Data on bedrock lithology and structure; properties of colluvium and residuum; slope aspect, steepness and profile; and rainfall during the storm are being digitized for use as independent variables in a multivariate modeling procedure to determine factors significantly correlated with landslide susceptibility.

During 1984 in Windsor County of central Vermont, heavy seasonal rainfall and melting of a thick snowpack triggered earthflows, slumps, and earth-block slides in Pleistocene surficial materials. Baskerville and Ohlmacher (1988) documented these landslides and studied the relation between the slope failures and properties of the geologic materials. Investigation of rock falls and rock block slides in the northern Appalachian Mountains of Vermont was undertaken to better understand the processes and the conditions leading to failure (Baskerville and others, 1988). Site specific monitoring studies were initiated to quantify and correlate climatic events and slope deformation rates in foliated and jointed metamorphic rocks (Lee, 1989).

In November of 1985, a storm in the central Appalachian

Mountains of Virginia and West Virginia triggered more than a 1000 shallow landslides in thin colluvium and residuum on shale slopes within a 1040 square kilometer study area (Jacobson, 1989a). Climatic conditions and the relative importance of land cover, bedrock and surficial geology, and geomorphology to location of landslide initiation were examined. Rainfall thresholds for the triggering of landslides were identified for individual geologic units (Jacobson and others, 1989a).

In the western United States recent studies of landslide processes have been conducted in Utah, California, Alaska and Hawaii. In both 1983 and 1984, heavy autumn rains, exceptionally thick winter snow packs, and sudden warming triggered abundant landslides along the Wasatch Front and on the Wasatch Plateau of Utah. The climatic, hydrologic, geologic and topographic conditions where landslides initiated were closely examined for better understanding of landslide processes and for improving landslide hazard zonation techniques (Baum and Fleming, 1989; Wieczorek and others, 1989).

Regional and topical studies of landslide processes in the San Francisco Bay region of California over several decades provided a background for developing landslide prediction techniques. Following detailed documentation of landslide location, timing and rainfall in the January 1982 storm (Ellen and Wieczorek, 1988), a regional landslide warning system was developed and first utilized to issue a warning during storms of February 1986. This system was based on empirical and analytical relations between rainfall and landslide generation, monitoring of regional rainfall data from telemetry rain gages, United States National Weather Service precipitation forecasts, and delineation of areas susceptible to landslide generation (Keefer and others, 1987).

To provide better calibration for rainfall-induced landslide triggering relations, an analytical model was developed, based on measured piezometric response to depict the influence of intense rainfall on pore pressures within a hillslope (Wilson, 1989); other improvements in the landslide warning system have also been undertaken (Wieczorek and others, 1990). Detailed monitoring of porewater pressures from instrumented slopes in Utah and California detected an abrupt drop in pore pressure immediately before failure of the slopes. This observation has potential application in future landslide hazard warning systems (Harp and others, 1990).

A cooperative project between the U.S. Geological Survey and the State of Alaska Division of Geological and Geophysical Surveys undertook investigations of the landslides which occurred during the March 27, 1964, Prince William Sound, Alaska earthquake. Geotechnical studies in and around Anchorage, Alaska, identified a sensitive silty clay facies of the

Bootlegger Cove Formation which, when subjected to seismic shear stresses, exhibited rapid strength reduction and was responsible for all the major Anchorage landslides during the 1964 earthquake which had previously been attributed to liquefaction of sandy facies (Updike and Carpenter, 1986; Updike and others, 1988 a,b).

In Honolulu, Hawaii, a study of the mechanics of slow-moving landslides using surface and subsurface testing, instrumentation and monitoring is being conducted to develop new methods of hazard mitigation (Baum and others, 1989; Baum and Fleming, in press). Maps of debris-flow hazards are being prepared for parts of Honolulu based on field mapping of deposits and utilizing computer runout models. Field instrumentation of rainfall and shallow ground-water levels at several sites, combined with hydrologic analyses, are being used to develop rainfall thresholds for a landslide warning system similar to the San Francisco Bay region, California.

LANDSLIDE SUSCEPTIBILITY AND RISK MAPPING

Accurate maps of regional and State landslide hazards are a prerequisite to a successful landslide hazards reduction. Information on the location and magnitude of landslide activity, and the susceptibility to future landslide movement, must be available to effect improved land-use planning, engineering design and construction, and warning and emergency response. Beginning informally in 1982, and augmented from 1985 through 1987 by a cooperative Federal-State landslide program, the USGS encouraged State geological surveys to prepare landslide inventory maps (e.g. Rheems and others, 1987), to formulate state landslide hazard mitigation plans (e.g. Jochim and others, 1988), and to undertake special investigations of specific landslides or geologic units prone to landsliding (e.g. Amos and Sandford, 1987).

As a prototype, a State landslide susceptibility map of Maryland was prepared with categories of susceptibility that were based on professional engineering geologic judgement and field experience of slope stability in individual mapped geologic units (Pomeroy, 1988). In order to develop and test new techniques for preparing State susceptibility maps, Brabb and others (1989) prepared a regional landslide inventory map for northern New Mexico. Geographic Information Systems (GIS) technology is being employed with digitized data on 127 geologic units along with slope and landslide inventory data to develop models for evaluating the probability of landsliding and to assist in the systematized preparation of landslide susceptibility maps for New Mexico.

In a study of landslide hazards in Cincinnati, Ohio, Bernknopf and others (1988) demonstrated that the economic costs and benefits of different mitigation strategies could be used as the basis for land use decisions. To evaluate the spatial distribution of expected landslide losses in the Cincinnati study area, regional geologic and topographic information was used to establish a regression equation that estimated the probability of landslide occurrence in 100-m square units. The probabilistic assessment of landslide susceptibility provides an essential tool for economic evaluation of community-imposed requirements for landslide hazard mitigation.

Several methods have recently been developed for assessing seismically-induced landsliding on a regional scale. A seismic slope stability map of San Mateo County in northern California, was developed from an analysis of potential landslide displacement during different characteristic earthquakes as a function of regional bedrock geology, slope, and ground-water levels (Wieczorek and others, 1985). In the Los Angeles region of southern California, the areal limits of landsliding from a postulated earthquake were assessed using a different technique incorporating theoretical and historical-empirical studies of distances from earthquake sources at which different landslide types occurred (Wilson and Keefer, 1985; Keefer and Wilson, 1989). In this method, the distance limit of earthquake-induced landslides from 40 historical earthquakes worldwide was used to determine an outer bound limit of distance as a function of earthquake magnitude. The Arias intensity, a measure of the severity of seismic shaking, that accounts for both strength and duration of shaking, was used to develop probability estimates for exceeding an Arias intensity threshold for triggering landslides at a particular distance from an earthquake source. In other ongoing work, Harp (this volume) is using strong-motion records and landslide distribution from several recent earthquakes to refine the use of Arias intensity thresholds for landsliding.

LANDSLIDE RECURRENCE AND SLOPE EVOLUTION

In early 1974, the upper part of the Manti landslide near Manti, Utah began moving and a little more than a year later, movement extended the full 3 km length of the old dormant landslide. Investigations into the history of the reactivation were undertaken including determining the rates of landslide enlargement and displacement (Fleming and others, 1988a); the physical properties and mode of failure of the landslide (Fleming and others, 1988b); and the hydrologic changes associated with the landslide movement (Williams, 1988).

Additional investigations of the Manti landslide are underway using a variety of Quaternary dating techniques to study the influence of short-term climatic change on slope failure. The influence of short- and long-term climatic changes on rates, processes, and geographic distribution of landslide activity will be examined elsewhere to better understand climatic influence on landslide recurrence.

Detailed measurement of movement and deformation has begun on the actively moving Slumgullion landslide near Lake City, Colorado. One of the purposes of the work is to improve quantitative methods of evaluation of hillslope stability and to predict enlargement and changes in rates of movement of landslides. Field and aerial photographic measurements of precise size, shape, and position of various movement features indicate, in addition to changes in rate and size, the potential options for stabilization (Baum and others, 1989). Additional investigations of the Slumgullion landslide will also provide new information on the response of large landslides to climate change. The Slumgullion landslide, like many other large landslides worldwide (Schuster, 1986), formed a prehistoric landslide dam that could provide information in the sedimentologic record for determining the climatic influence on landslide movement.

Studies of the surficial stratigraphic record of the central Appalachians in the eastern United States by Jacobson and others (1988b) have revealed a profound climatic influence on slope processes. Most of the region exhibits multiple, prominent hillslope and alluvial terrace deposits indicative of climate changes with durations and recurrence frequencies of tens of thousands of years or more. Holocene catastrophic events have only caused minimal erosion of these features that appear to be associated with a very different climate in the Pleistocene (Jacobson and others, 1989b).

RESEARCH APPLICATIONS AND TECHNOLOGY TRANSFER

The USGS is working to provide private individuals, commercial and industrial establishments, and local, State and Federal government institutions with the information to evaluate systematically the level of landslide hazard to which they are exposed. The USGS transfers landslide susceptibility maps and risk assessments, regional and local landslide prediction procedures and methodologies, and results of landslide research. As a direct form of research application and technology transfer, the USGS provided assistance to Federal, State, county, and local agencies during recent landslide disasters in the San Francisco Bay region (1982, 1986, and 1989); in Utah (1983, 1984); in Puerto Rico (1985); in Virginia, West Virginia (1985); and in Hawaii (1988). The assistance in these cases has ranged from short-term, post-disaster reconnaissance studies with immediate mitigation recommendations to several-year long projects involving intensive investigations and development of comprehensive mitigation plans. For example, a 1- to 2-year, program of studies of landslides caused by the October 17, 1989, Loma Prieta earthquake, was funded by the Federal Emergency Management Agency, and cooperatively directed by the USGS, U.S. Corps of Engineers, State of California-Division of Mines and Geology, County of Santa Cruz, and University of California at Santa Cruz. The results of these studies will influence land-use regulations on landslide-prone terrain in Santa Cruz County, California.

To improve technology transfer, the USGS is developing a National Landslide Information Center (NLIC) in Denver, Colorado. The NLIC will be a multi-functional enterprise dedicated to the collection and distribution of all forms of information related to landslides-- data from landslide monitoring projects, digital data files of landslide inventories, and geographical information system (GIS) digital representation of landslide susceptibility and risk, as well as traditional published maps, reports, and books. Over the next decade the NLIC will be devolved to serve landslide researchers, geotechnical practitioners engaged in landslide stabilization, and all other people and entities concerned in any way with landslide hazard analysis and mitigation.

REFERENCES

Amos, J., and Sandford, T.C., 1987, Landslides in the Presumpscot Formation, Southern Maine: Maine Geological Survey, Open-file no. 87-4, 68p.

Baskerville, C.A., and Ohlmacher, G.C., 1988, Some slope-movement problems in Windsor County, Vermont: U.S. Geological Survey Bulletin 1828, 25p.

Baskerville, C.A., Ratte, C.A., and Lee, F.T., 1988, A rockfall and debris slide at Smugglers Notch: Studies in Vermont Geology No. 4, 9p.

Baum, R.L., and Fleming, R.W., in press, Longitudinal forces in landslides--a comparison between field observations and a one-dimensional model: submitted to the Geological Society of America Bulletin, 35p.

Baum, R.L., and Fleming, R.W., 1989, Landslides and debris flows in Ephraim Canyon, Central Utah: U.S. Geological Survey Bulletin 1842-C, p. C1-C11.

Baum, R.L., Fleming, R.W., and Ellen, S.D., 1989, Map showing landslide features and related ground deformation in the Woodlawn area of the Manoa Valley, City and County of Honolulu, Hawaii: U.S. Geological Survey Open-File Report 89-290, 16p.

Bernknopf, R.L., Campbell, R.H., Brookshire, D.S., and Shapiro, C.D., 1988, A probabilistic approach to landslide hazard mapping in Cincinnati, Ohio, with applications for economic evaluation: Bulletin of the Association of Engineering Geologists, v. 25, n.1, p. 39-56.

Brabb, E.E., Guzetti, F., Mark, R., and Simpson, R.W., 1989, The extent of landsliding in northern New Mexico and similar semi-arid and arid regions: in Sadler, P.M. and Morton, D.M., eds., Landslides in a Semi-arid Environment: Publication of the Inland Geological Society, v.2, Riverside, California, p. 163-173.

Ellen, S.D., and Wieczorek, G.F., 1988, Landslides, floods, and marine effects of the storm of January 3-5, 1982, in the San Francisco Bay region, California: U.S. Geological Survey Professional Paper 1434, 310p.

Fleming, R.W., Johnson, R.B., and Schuster, R.L., 1988a, The reactivation of the Manti landslide, Utah: in The Manti, Utah, Landslide, U.S. Geological Survey Professional Paper 1311-A, 22p.

Fleming, R.W., Schuster, R.L., and Johnson, R.B., 1988b, Physical properties and mode of failure of the Manti landslide, Utah: in The Manti, Utah, Landslide, U.S. Geological Survey Professional Paper 1311-B, 23-42.

Harp, E.L., Wells, W.G.III, and Sarmiento, J.G., 1990, Pore pressure response during failure in soils: Geological Society of America Bulletin, v. 102, p. 428-438.

Jacobson, R.B., Cron, E.D., and McGeehin, J.P., 1989a, Slope movements triggered by heavy rainfall, November 3-5, 1985, in Virginia and West Virginia, U.S.A.: in Schultz, A.P., and Jibson, R.W., eds., Landslide Processes of the eastern United States and Puerto Rico: The Geological Society of America Special Paper 236, Boulder, Colorado, p. 1-14.

Jacobson, R.B., Miller, A.J., and Smith, J.A., 1989b, The role of catastrophic geomorphic events in central Appalachian landscape evolution: Geomorphology, Elsevier, v. 2, p. 257-284.

Jibson, R.W., 1989, Debris flows in southern Puerto Rico: in Schultz, A.P., and Jibson, R.W., eds., Landslide Processes of the eastern United States and Puerto Rico: The Geological Society of America Special Paper 236, Boulder, Colorado, p. 29-56.

Jochim, C.L., Rogers, W.P., Truby, J.O., Wold, R.L.Jr., Weber, G., and Brown, S.P., 1988, Colorado Landslide Hazard Mitigation Plan: Colorado Geological Survey, Department of Natural Resources, Denver, Colorado, Bulletin 48, 149p.

Keefer, D.K., Wilson, R.C., Mark, R.K., Brabb, E.E., Brown, W.M. III, Ellen, S.D., Harp, E.L., Wieczorek, G.F., Alger, C.S., and Zatkin, R.S., 1987, Real-time landslide warning during heavy rainfall: Science, v. 238, pp.921-925.

Keefer, D.K., and Wilson, R.C., 1989, Predicting earthquake-induced landslides, with emphasis on arid and semi-arid environments: in Sadler, P.M. and Morton, D.M., eds., Landslides in a Semi-arid Environment: Publication of the Inland Geological Society, v.2, Riverside, California, p. 118-149.

Lee, F.T., 1989, Slope movements in the Cheshire Quartzite, southwestern Vermont: in Schultz, A.P., and Jibson, R.W., eds., Landslide Processes of the eastern United States and Puerto Rico: The Geological Society of America Special Paper 236, Boulder, Colorado, p. 89-102.

Pomeroy, J.S., 1988, Map showing landslide susceptibility in Maryland, U.S. Geological Survey Miscellaneous Field Studies Map MF-2048, 8p.

Rheams, K.F., Brabb, E.E., and Taylor, F., 1987, Preliminary map showing landslides in Alabama: U.S. Geological Survey Miscellaneous Field Studies Map, MF 1954.

Schuster, R.L., ed., 1986, Landslide Dams: Processes, Risk, and Mitigation, American Society of Civil Engineers, Geotechnical Special Publication No. 3, 164p.

Updike, R.G., and Carpenter, B.A., 1986, Engineering geology of the Government Hill area, Anchorage, Alaska: U.S. Geological Survey Bulletin 1588, 32p.

Updike, R.G., Egan, J.A., Moriwaki, Y., Idriss, I.M., Moses, T.L., 1988a, A model for earthquake-induced translatory landslides in Quaternary sediments: Geological Society of America Bulletin, v. 100, p. 783-792.

Updike, R.G., Olsen, H.W., Schmoll, H.R., Kharaka, Y.K., and Stokoe, II, 1988b, Geologic and geotechnical conditions adjacent to the Turnagain Heights landslide, Anchorage, Alaska: U.S. Geological Survey Bulletin 1817, 40p.

Wieczorek, G.F., Lips, E.W., and Ellen, S.D., 1989, Debris flows and hyperconcentrated floods along the Wasatch Front, Utah, 1983 and 1984: Bulletin of the Association of Engineering Geologists, v. 26, p. 191-208.

Wieczorek, G.F., Wilson, R.C., and Harp, E.L., 1985, Map of slope stability during earthquakes in San Mateo County, California: U.S. Geological Survey Miscellaneous Investigations Map I-1257-E, scale 1:62,500.

Wieczorek, G.F., Wilson, R.C., Mark, R.K., Keefer, D.K., Harp, E.L., Ellen, S.D., Brown, W.M.III, and Rice, P., 1990, Landslide warning system in the San Francisco Bay region, California: Landslide News, Japan Landslide Society, n. 4, July 1990, p.5-8.

Williams, G.P., 1988, Stream-channel changes and pond formation at the 1974-76 Manti landslide, Utah, in The Manti, Utah, Landslide, U.S. Geological Survey Professional Paper 1311-C, p. 43-69.

Wilson, R.C., 1989, Rainstorms, pore pressures, and debris flows: a theoretical framework: in Sadler, P.M. and Morton, D.M., eds., Landslides in a Semi-arid Environment: Publication of the Inland Geological Society, v.2, Riverside, California, p. 101-117.

Wilson, R.C., and Keefer, D.K., 1985, Predicting areal limits of earthquake-induced landsliding: in Ziony, J.I., ed., Evaluating earthquake hazards in the Los Angeles region- An earth-science perspective, U.S. Geological Survey Professional Paper 1360, p. 317-338.

Figure 1- Locations of landslide studies referred to within text. Alaska, Hawaii and Puerto Rico are not shown in proper geographic location. In order of discussion in text: 1) Puerto Rico, 2) Windsor, Vermont, 3) central Appalachian mountains of Virginia/West Virginia, 4) Wasatch Front and Plateau of Utah, 5) San Francisco Bay region, California, 6) Anchorage, Alaska, 7) Honolulu, Hawaii, 8) Maryland, 9) New Mexico, 10) Cincinnati, Ohio, 11) San Mateo, California, 12) Los Angeles, California, 13) Manti, Utah, and 14) Lake City, Colorado.

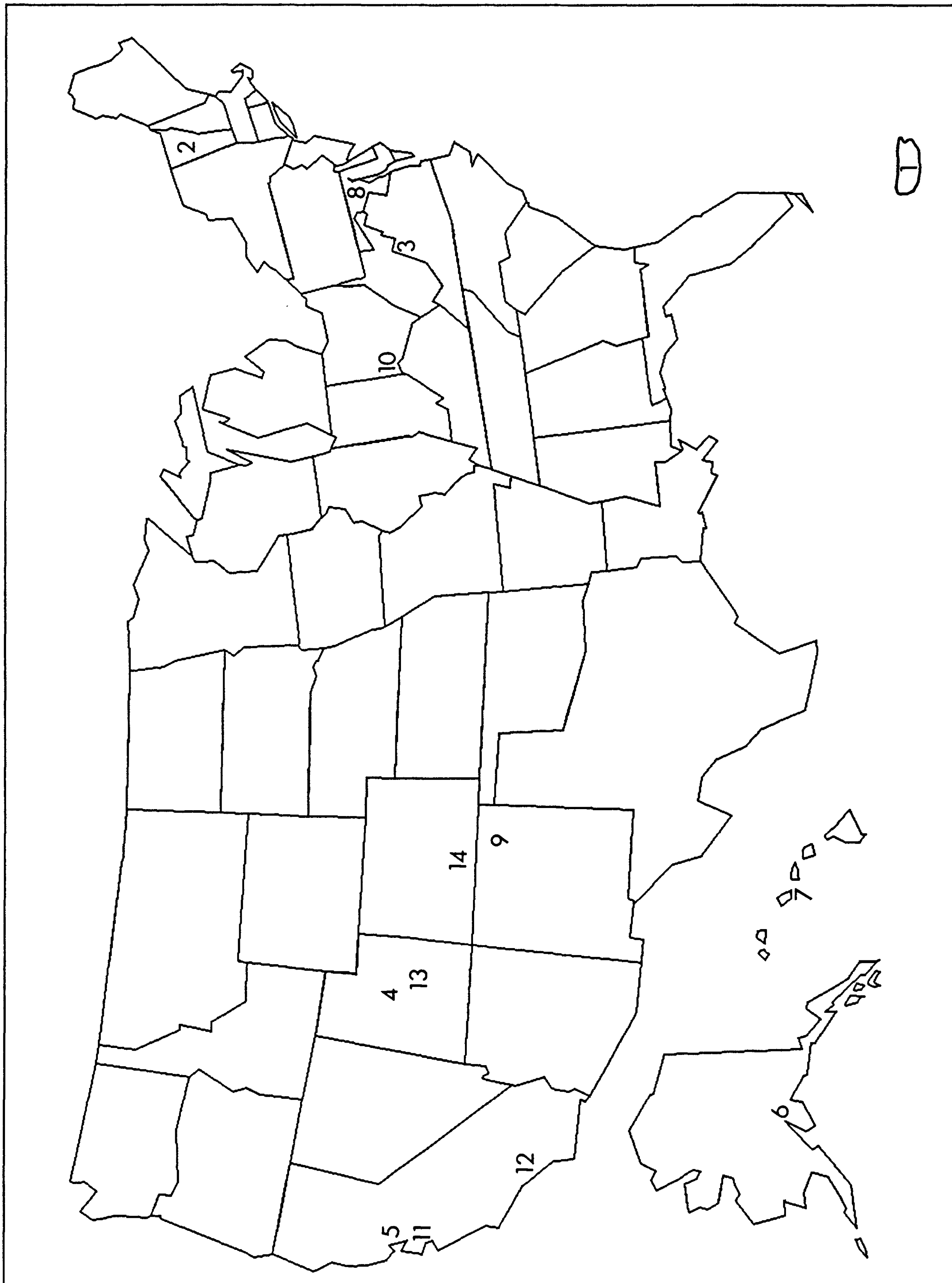

Figure 1

LANDSLIDE DAMS -- HAZARDS AND MITIGATION

by

Robert L. Schuster

INTRODUCTION

Landslide dams significantly affect the morphologies of valleys by changing valley gradients and often causing significant deposition of fine sediments in the impoundments. Catastrophic failures result in hazards to people and development in many parts of the world. These factors must be considered when locating engineered structures, such as hydroelectric dams, in valleys in which landslide dams have occurred or have the potential to occur (Schuster and Costa, 1986).

Because they lack controlled outlet structures, nearly all landslide dams eventually are overtopped by their impounded lakes, and many have failed catastrophically, causing major downstream flooding (Costa and Schuster, 1988). Casualties from some of these floods have reached into the many thousands. The worst known case occurred in 1786 when a landslide dam of the Dadu River in Sichuan Province, China, breached; the resulting deluge extended 1,400 km downstream, drowning as many as 100,000 people (Li, 1989). In another extreme example, the 1841 failure of a 200-m-high landslide dam of the Indus River, India, caused a disastrous flood of water and mud that swept away hundreds of villages and towns with great numbers of casualties (Mason, 929).

CHARACTERISTICS OF LANDSLIDE DAMS

GEOMORPHIC SETTINGS

Steep-walled, narrow valleys in high rugged mountains commonly are the sites of the highest landslide dams because (1) these valleys are subject to slope failure and (2) their cross sections are such that they require relatively small amounts of material to form blockages. Mountain valleys can also be the sites of low dams; a common case is the formation of a low dam on a river by a debris flow or mudflow issuing from one of its tributaries.

TYPE OF LANDSLIDES THAT CAUSE DAMMING

The vast majority of landslide blockages is caused by (1) rock and soil slumps and slides, (2) rock and debris avalanches, and (3) debris flows and mudflows. A few have been caused by slope failures in sensitive clays and by rock and earth falls.

CAUSES OF DAM-FORMING LANDSLIDES

The most important causes of initiation of landslides that form dams are abnormally high precipitation (including rapid snow melt) and earthquakes. Landslide damming is so common following major earthquakes that "dammed lakes" are specifically noted under Intensity XII of the Modified Mercalli Intensity Scale of 1931 (Wood and Neumann, 1931).

SIZE AND GEOMETRY

Landslide dams range in height from only a few meters to hundreds of meters high. The highest (800-m) landslide dam known to have occurred during historic time was caused by the 1911 earthquake-triggered 2.5-km^3 Usoy rock avalanche, which dammed the Murgab River in the south-central U.S.S.R., forming 53-km-long Sarez Lake (Berg, 1950). The Usoy landslide dam is more than twice as high as the world's largest constructed dam, 300-m-high Nurek earth-fill dam, also in the south-central U.S.S.R.

For each landslide dam more than 10-20 m high, there are many that are only 1-2 m high. Most of the low dams fail within a few hours or days and many of them are never observed. A high percentage of these small dams are formed by debris flows from tributary streams.

Landslide dams commonly differ from constructed earth-fill dams in material volume and in the relationship between height of the blockage and its width (dimension parallel to the stream). Landslide dams commonly are much wider than earth-fill dams of the same height, and thus involve considerably larger volumes.

MODES OF FAILURE OF LANDSLIDE DAMS

Landslide-dammed lakes may last for several minutes or for several thousand years, depending on many factors, including: (1) volume and rate of water and sediment inflow to the newly formed lake, (2) size and shape of the dam, (3) geotechnical properties of the geologic materials comprising the dam, and (4) rates of seepage through the blockage. Failure of landslide dams depends on resistance to erosion, either at the dam surface from surface-water runoff, or inside the dam due to seepage. Landslide dams consisting of large rock fragments or cohesive particles resist failure more successfully than dams containing large percentages of soft rock or unconsolidated geologic materials. Landslide dams composed mainly of soft, low-density, fine-grained, or easily liquefied materials are hazardous because they are relatively susceptible to erosion.

Because of the lack of erosion-resistant outlets, landslide dams commonly fail by overtopping followed by rapid surface erosion, progressing from the toe of the dam toward the crest. Because of "self armoring" of the eroding outlet (a process involving removal of fine material by the water, which leaves coarser, erosion-resistant fragments in the channel), the breach in many cases does not erode down to the original river level. For this reason, smaller lakes often remain after dam failure.

In a few cases, landslide-dammed lakes have formed natural spillways across adjacent bedrock abutments. These spillways prevent overtopping and possible breaching of the dams. This process may occur where the toe of the landslide dam is higher than the surface of the adjacent bedrock abutment.

FLOODS FROM LANDSLIDE DAMS

Landslide dams create the potential for two very different types of flooding: (1) upstream (backwater) flooding as the lake fills and (2) downstream flooding due to failure of the dam. The threat of loss of life from upstream flooding is minimal, but property damage can be substantial. Important facilities, such as hydroelectric power plants, may become inoperable (Schuster and Costa, 1986). Although less common than upstream flooding, downstream flooding from failure of landslide dams is generally a more serious problem. A catastrophic example of downstream flooding resulted from the A.D. 1515 failure of a rock-avalanche blockage of the Brenno River, a tributary of the Ticino River, in southern Switzerland. The flood engulfed the city of Biasca with an explosive surge of debris and water that continued down the Ticino valley for 35 km to Lake Maggiore on the Italian border (Montandon, 1933, pp. 295-296). About 600 people were killed by the flood.

ENGINEERED CONTROL MEASURES

The simplest and most commonly used method of improving the stability of a landslide dam has been the construction of protected spillways either across adjacent bedrock abutments or over the dam itself. An example of a carefully engineered spillway across a landslide dam was constructed by the U.S. Army Corps of Engineers on the 1959 Madison Canyon landslide dam, Montana, U.S.A. This 75-m-wide spillway was designed for a discharge of 280 m^3/s and velocities that would only slowly erode the rock sizes that comprised the surface of the landslide dam (Harrison, 1974).

In a few cases, large-scale blasting has been used to excavate new stream channels through landslide dams. This technique was used in 1964 to open a channel through a 15-million-m^3 landslide that dammed the Zeravshan River in Tadzhikistan, U.S.S.R., upstream from the ancient city of Samarkand (Engineering News-Record, 1964). The dam was 220 m high, 400 m long, and more than 1800 m wide. Two blasts, utilizing 250 tons of explosives, successfully excavated 230,000 m of landslide material and formed a 40-to-50 m-deep drainage channel through the blockage.

Other methods of preventing overtopping of landslide dams by stabilizing lake levels include drainage through gravity and siphon pipes, pumping systems, and tunnel outlets and diversions. A system of siphons and pumps was used to drain the lake formed by the damming of the Adda River in northern Italy by a large rock slide/rock avalanche in 1987 (Govi, 1989). In 1988, flow through the Adda River was diverted through two bedrock tunnels

(6.0 and 4.2 m in diameter) constructed through the left abutment of the dam.

REFERENCES

Berg, L. S., 1950, Natural regions of the U.S.S.R.: New York, Macmillan Co., 435 p.

Costa, J. E., and Schuster, R. L., 1988, The formation and failure of natural dams: Bulletin of the Geological Society of America, v. 100, p. 1054-1068.

Engineering News-Record, 1964, Russians blast through landslide dam: 7 May, p. 24.

Govi, M., 1989, The 1987 landslide on Mount Zandila in Valtellina, northern Italy: Landslide News, Japan Landslide Society, no. 3, p. 1-3.

Harrison, A., 1974, Madison Canyon slide mass modification by the U.S. Army Corps of Engineers, in Voight, B., ed., Rock mechanics - the American Northwest: Third International Congress on Rock Mechanics, International Society for Rock Mechanics, Pennsylvania State University College of Earth Sciences Experiment Station Special Publication, p. 138-143.

Li Tianchi, 1989, Landslides: extent and economic significance in China, in Brabb, E. E., and Harrod, B. L., eds., Landslides: extent and economic significance: Proceedings of 28th International Geological Congress, Symposium on Landslides, Washington, D.C., 17 July, p. 271-287.

Mason, K., 1929, Indus floods and Shyok glaciers: The Himalayan Journal, v. 1, p. 10-29.

Montandon, F., 1933, Chronologie des grands eboulements alpins, du debut de l'ere chretienne a nos jours, in Materiaux pour l'Etude des Calamites. Societe de Geographie Geneve, v. 32, p. 271-340.

Schuster, R. L., and Costa, J. E., 1986, Effects of landslide damming on hydroelectric projects: Proceedings of 5th International Congress of the International Association of Engineering Geology, Buenos Aires, 20-25 October, v. 4, p. 1295-1307.

Wood, H. O., and Neumann, F., 1931, Modified Mercalli Intensity Scale of 1931: Seismological Society of America Bulletin, v. 21, no. 4, p. 277-283.

INSTRUMENTAL SHAKING THRESHOLDS FOR SEISMICALLY INDUCED LANDSLIDES
AND
PRELIMINARY REPORT ON LANDSLIDES TRIGGERED BY THE OCTOBER 17, 1989, LOMA PRIETA, CALIFORNIA EARTHQUAKE

by

Edwin L. Harp

INTRODUCTION

It has long been recognized that landslides triggered by earthquakes often account for the major portion of damage and loss of life in earthquakes rather than damage and destruction resulting directly from the shaking or primary faulting. Examples such as the giant debris avalanche shaken loose from the slopes of Mt. Huascaran in the M 7.9 Peru earthquake of 1970, the rock slide created by the 1959 Hebgen Lake earthquake in southwestern Montana, or the rock avalanche triggered by the 1984 Nagano Ken Seibu earthquake in Japan serve to emphasize the fact that just one landslide can dominate the entire earthquake hazard scenario of a region.

INSTRUMENTAL SHAKING INTENSITY THRESHOLDS

Because the generation of seismically induced landslides depends on the characteristics of shaking as well as the mechanical properties of geologic materials, it is critical to understand as much as possible about the variation in ground shaking in an earthquake. The most numerous types of landslides generated in earthquakes, rock falls, rock slides, soil falls, and soil slides are extremely sensitive to shaking levels, and their initiation has been correlated with Modified Mercalli Intensity levels of shaking (Keefer, 1984, Harp and others, 1981, Wilson and Keefer, 1985).

Until recently, the data most often available on the patterns of shaking intensity from an earthquake were MMI contours prepared from observations of damage to structures and utilities. Even now, in most earthquakes, there is a scarcity of instrumental strong-motion data, especially in the near field. Although MMI data is commonly available from most earthquake investigations, its use in determining the detailed variations of strong shaking from an earthquake is of limited value. MMI values assigned by investigators are qualitative and interpretive, based on observations and are often subjective and observer-dependent.

Where strong-motion data exist, we prefer to use an intensity based on a strong-motion accelerogram. Arias intensity, or I_a, was originally defined by Arias (1970). Arias intensity is defined as an integration over time of the acceleration squared from an accelerogram:

$$I_a=\pi/2g\int_0^\infty [a(t)]^2 dt$$

where a is acceleration, t is time, and g is the acceleration of gravity. Arias intensity is expressed in units of velocity, usually m/sec. Because the calculation of Arias intensity involves the entire record, the value is proportional to the duration of the shaking record as well as the amplitude. I_a is generally calculated from one of the horizontal components of the accelerogram. To eliminate a directional bias from one of the components being much larger than the other, we sum the respective I_a values of both components to produce I_h.

PREVIOUS USE OF ARIAS INTENSITY TO ESTIMATE LANDSLIDE EFFECTS

Using arguments regarding the critical acceleration thresholds for different general classes of landslides, Wilson and Keefer (1985) calculated Arias intensity thresholds for landslides of different types. For rock falls and other disrupted failures, this was determined to be approximately I_h = 0.25 m/sec. Then, using seismograms from earthquakes in southern California, they calculated the distribution of this Arias intensity threshold in terms of magnitude and distance away from seismic source. Worldwide landslide data (Keefer, 1984) plotted in terms of farthest distance from source versus magnitude was then compared with the magnitude-distance threshold plot of Arias intensity and found to be similarly distributed.

Having a theoretical relationship between Arias intensity, magnitude, and distance, we can then predict how far away from the seismic source that landslides are likely to occur for a given magnitude earthquake in terms of the probability of shaking exceeding the critical Arias intensity necessary for landslide initiation. Given a vertical strike-slip fault typical of the San Andreas system in California, the limits for the exceedance of critical Arias intensity levels are symmetrically located ellipses with respect to the source zone projected on the earth's surface. In reality, the locus of landslide limits from earthquakes are seldom symmetrical but are highly asymmetric with respect to the source because of variations in geologic materials and their respective susceptibility to failure and the variation in shaking caused by the seismic source itself and/or differences in shaking levels due to site response.

The first two earthquakes to give us real data to correlate Arias intensity values with landslide (rock fall) thresholds were the October 1, 1987 Whittier Narrows earthquake (M = 6.1) and the November 24, 1987 Superstition Hills earthquake (M = 6.6), both in southern California.

The magnitude 6.6 earthquake in the Superstition Hills produced an Arias intensity distribution that was, as we expected, less symmetrical with respect to the source area than theory predicted. However, when compared to the areal limit of landslides, revealed an intensity range for the threshold of landslides that is consistent with the theory. The range of I_h for the triggering level of rock falls in this earthquake was $I_h \approx 0.2-0.9$ m/s.

The Whittier Narrows earthquake produced a much more complicated picture of the Arias intensity threshold for landslides. Here, there were two threshold ranges, one of $I_h \approx 0.42-0.47$ m/s and $I_h \approx 0.02-0.07$ m/s, the latter approximately an order of magnitude lower than that from the Superstition Hills earthquake.

Subsequent field investigation has established that the most obvious explanation for this dual threshold is that the threshold level of Arias intensity depends on site effects, particularly the fracture characteristics of the outcrops present. The lithology in areas of the higher threshold is made up of Miocene and Pliocene sandstone, shale, and conglomerate with relatively tight fractures. Although these deposits are relatively uncemented and present in steep slopes, the fractures having few large openings resulted in the higher Arias intensity threshold. In areas where the lower threshold occurred, the rocks ranged from Mesozoic sandstone and conglomerate to Precambrian (Archean) gneisses and schists with relatively loose open fractures and large quantities of loose rock as talus on slopes. Although these older rocks are harder, better cemented and more indurated, the large aperture of the fracture systems gives them a higher susceptibility to earthquake-induced rock fall and a lower threshold of Arias intensity.

As additional data becomes available from other earthquakes, we will be able to refine our data to more precise ranges of Arias intensity and have a more complete picture of its variation with respect to different rock types. We also anticipate defining Arias intensity levels for various general types of landslides.

SEISMICALLY INDUCED LANDSLIDES FROM THE LOMA PRIETA EARTHQUAKE

The M = 7.1, October 17, 1989, earthquake that struck the San Francisco Bay region triggered thousands of landslides over an area of 14,000 km^2. This region contains most of the San Francisco Bay area, the Santa Cruz and Monterey Bay area, nearby portions of the California Coast Ranges, and the coastline up to 130 km south of the epicenter. As well as causing over $10 million of damage to utilities, housing, and other structures, landslides blocked roads closing lifelines and hampering rescue efforts.

Landslides were most concentrated near the earthquake source in the heavily vegetated Santa Cruz Mountains, which had previously produced abundant landslides during years of heavy rainfall in winter storms. Landslides were numerous from this earthquake in spite of its occurrence at the end of a two-year drought period.

The most numerous types of landslides triggered were rock falls, rock slides, and soil slides that were typically smaller than 100 m^3 although some had volumes of between 1,000 and 10,000 m^3. Highway 17, between Los Gatos and Santa Cruz, a major avenue for commuters in the San Francisco Bay area, was closed for over a month by two rock falls.

Deeper seated block slides and rotational slumps, with failure surfaces possibly as deep as 70 m occurred in high concentrations along the south flank of Summit Ridge between Highway 17 and Highland Road. The top of Summit Ridge, which extends approximately east-west is occupied by Summit Road, a major access road for residents in the area. This and other roads as well as over 70 houses were heavily damaged by these landslides and other coseismic fissuring.

This area of deep-seated landslides and fissures lies immediately to the southwest of the surface trace of the San Andreas fault zone, and its center is approximately 10 km northwest of the earthquake epicenter. The network of fractures formed during the earthquake dissected the Summit Ridge area in complicated way. The complex pattern produced by the landslides and other fractures presented a confusing picture to geologists who were unable to recognize primary surface faulting along the surface trace of the San Andreas fault itself. Instead of a clear zone of right lateral shear fractures, there was a zone up to 5 km wide in which fractures were left lateral, right lateral, extensile, normal, thrust, and combinations of these, mixed with what were, in some cases, clearly identifiable landslides.

A majority of the fractures with shear displacement showed left lateral offset. Fractures tended to be discontinuous. Fractures of several meters depth and up to 1.0 m of displacement seldom extended for more than 400 m. The majority of fractures showed extension to the dominant component of the total displacement. Fractures trending N40-80W tend to be parallel to bedding and/or regional faults. Therefore, fractures falling within this trend range are interpreted as being tectonic or related to regional structure rather than landslide related unless clearly associated with a landslide feature. Numerous other fractures form headwall scarps and lateral shear margins of deep-seated rotational slumps or block slides (landslide nomenclature is that of Varnes, 1978).

Fractures and fissures interpreted as being of tectonic origin include cracks located along linear ridge-top depressions and linear fractures that extend across well-defined landslide features. Some of these may have resulted from shear displacement along bedding planes of steeply dipping sandstone and shale formations (Cotton and others, 1990). Other fissures may have formed as extensional partings along bedding or joints within the underlying sedimentary formations. The presence of uphill-facing scarps along such fractures suggests a tectonic origin, although this relationship is not in itself conclusive. Some uphill-facing scarps may have been formed by lateral deformation of the summit ridge with resultant subsidence of a ridge-top trough (sackűng).

Most recognizable among landslide-related cracks are extension fractures, commonly located along preexisting headwall scarps. These fractures have the largest displacements of all the landslide-related cracks. Displacements across the scarps of the largest deep-seated slumps exceed 1.0 m, are extensional and valley side down, similar to a normal fault.

Fractures that formed lateral margins of landslides generally exhibit shear displacement consistent with the relative displacement of the landslide mass. There are, however, numerous areas where the relative displacement of the landslide is not clear and where the relation of the sense of displacement across individual cracks to the overall mass movement is also unclear. The least common deformational features related to earthquake-triggered landslides are well-defined folds or fractures along the toes of landslides of which only a few isolated small features were observed.

Extensional fractures along the crests of narrow, steep-sided ridge tops occurred in several areas within the epicentral area. The intense ridge-crest fracturing occurred approximately 6 km west of the epicenter on a steep ridge where wood frame houses were located along the ridge crest. Shaking was so violent here that walls were torn from houses and, in some cases, complete collapse of the dwelling ensued. Rocks, concrete slabs, and logs in this area were also found displaced from their original positions with little or no evidence of transport by rolling. These objects appear to have been thrown from their original positions to their present ones by vertical accelerations of over 1.0 g.

REFERENCES

Cotton, W. R., Fowler, W. L., and Van Velsor, J. E., 1990, Coseismic bedding-plane faults and ground fissures associated with the Loma Prieta earthquake of October 17, 1989,_in_ McNutt, S. R., and Sydnor, R. H., eds., The Loma Prieta "Santa Cruz" Mountains, California Earthquake of 17 October 1989: California Division of Mines and Geology Special Publication 104, p. 95-103.

Harp, Edwin L., Wilson, Raymond C., and Wieczorek, Gerald F., 1981, Landslides from the February 4, 1976, Guatemala earthquake: U.S. Geological Survey Professional Paper 1204-A, 35 p., 2 pl.

Keefer, David K., 1984, Landslides caused by earthquakes: Geological Society of America Bulletin, v. 95, p. 406-421.

Varnes, David J., 1978, Slope movement types and processes, in Schuster, Robert L., and Krizek, Raymond J., eds., Landslides Analysis and Control: Transportation Research Board Special Publication 176, National Academy of Sciences, p. 11-33, 1 pl.

Wilson, R.C., and Keefer, D.K., 1985, Predicting areal limits of earthquake-induced landsliding, in, Ziony, J.I., ed., Evaluating Earthquake Hazards in the Los Angeles Region- An Earth-Science Perspective: U.S. Geological Survey Professional Paper 1360, p. 317-345.

DEFORMATION OF LANDSLIDE SURFACES AS INDICATORS OF MOVEMENT PROCESSES

by

Robert W. Fleming[1], Rex L. Baum[1], and Arvid M. Johnson[2]

Studies of the deformation that occurs at the surface of a moving landslide can provide insight into landslide kinematics and stability analysis. The types of deformation that are useful to monitor include (1) cause, distribution, and growth of individual cracks and faults, (2) displacement of points on landslide surfaces, and (3) point measurement of strain on landslide surfaces (Baum, Johnson, and Fleming, 1988; Fleming and Johnson, 1989; Baum, Fleming, and Ellen, 1989). One example of measurements and observations is summarized here to illustrate applications of specific methods.

DEFORMATION AT THE TWIN LAKE LANDSLIDE, UTAH

The Twin Lake landslide is in Twelvemile Canyon, about 9 km east of the small town of Mayfield, Utah. The landslide, a reactivation of old landslide debris, began moving during the spring of 1983. Movement was initially rapid (as much as 10 m per day) through May and June, and amounts of movement locally exceeded 45 m. Movement stopped during the summer of 1983 but began again during the spring of 1984. Since 1984, the landslide has been dormant.

The Twin Lake landslide is about 450 m wide and 900 m long. Based on a thickness of 30 m determined by one boring, the volume is about 12 million m^3. During the period of rapid movement, the ground surface was relatively dry and brittle. As a result of movement, the ground was broken by a myriad of fractures, including faults and open cracks. The landslide is bounded on the west by strike-slip faults and on the east by a complex of strike-slip, normal, and thrust faults. The head of the landslide is north, and movement was toward the south.

Aerial photographs (scale 1:6,000) of the landslide were taken at three times--in May, 1983, just after movement had begun; in June 1983, after about three-fourths of the total movement had occurred; and in June 1984, after movement had ceased. Detailed maps of cracks and faults were prepared using photo enlargements and plane-table maps as bases. Figure 1 is a simplified map of the principal cracks and faults.

In the lower (south) part of the landslide, there are two prominent left-lateral strike-slip faults that divide the landslide toe into three separate elements. These strike-slip

[1]U.S. Geological Survey, Denver, Colorado 80225
[2]Purdue University, West Lafayette, Indiana 47907

faults are boundaries between landslide elements. Deformational patterns are different in each element. In the westernmost element, there are both normal and thrust faults. In the middle element, the entire lower part of the landslide is comprised of a series of subparallel thrust faults indicating that the landslide debris is being compressed throughout. The eastern element of the landslide toe also contains internal thrust faults, small buckle folds, and numerous discontinuous left-lateral faults that individually contain small displacements. Overall, the deformational pattern in the eastern element is compression and shearing.

Farther upslope, there is an area of thrust faults with most arranged arcuately across the mid-part of the landslide (fig. 1). Toward the west side, the thrust faults are intermingled with subparallel normal faults in a pattern that indicates both stretching and shortening are occurring in the same place. In the upper half of the landslide, the features are almost exclusively normal faults.

Displacement of the surface of the landslide was measured for about 150 points using an analytical stereoplotter and the three sets of aerial photography. Coordinates of photo-identifiable points were computed and displacement plotted as vectors on figure 2. Points off the slide are shown as open circles; measurement of these stable points revealed that displacements on the moving ground are accurate to about ± 1 m.

The scalar magnitudes of the displacement vectors have been used to draw a contour map of the displacement (fig. 2). Large offsets in displacement occur along the major internal boundaries in the toe. For example, note that there was about 30 m of differential displacement along the left-lateral fault just east of "A" in the shaded part of figure 2. Displacement in the shaded area represented by "A" increased from about 27 to 45 m and then decreased to zero at the toe. Similarly, in the shaded area "B" on figure 2, the displacement increases from a background value of about 12 m at the upslope end to a maximum of 36 m. Farther downslope, displacement decreased to 24-27 m at the thrust fault at the downslope end of "B".

These two shaded areas shown as "A" and "B" contain similar patterns of cracks and faults (fig. 1) as well as distinctive displacement patterns. Within each shaded area, extension occurs in the upper part and compression in the lower part. This deformation and crack pattern, together with the displacement record, identifies each area as a smaller landslide within the boundaries of the larger Twin Lake landslide.

The displacement pattern for the larger landslide can be isolated by removing the displacements of the smaller landslides. The amounts of displacement outside the shaded areas show consistent increases from the upslope end to the heads of the smaller landslides (fig. 2). Furthermore, there is consistent shortening in the area when displacement decreases from 21 to 0 m in the middle element of the toe. Extending the trends of these displacement contours of the larger Twin Lake landslide across the shaded areas in effect subtracts the additional displacement due to superimposed movement within the shaded areas "A" and "B" and greatly simplifies the displacement pattern (fig. 3). The amount of displacement of the Twin Lake landslide increased from 0 to about 24 m; then it decreased to 0 m at the toe.

Additional information about landslide kinematics can be extracted from the maps by comparison of the different data in figures 1, 2, and 3. For example, most displacement vectors are oriented normal to the scalar displacement contours. In these areas where the contours are at right angles to the displacement vectors, the distortion of the landslide debris is pure stretching or shortening.

The structures associated with stretching are tension cracks and normal faults that are common in the upper part of the landslide. Thrust faults and buckle folds characterize the shortening or compression evident in the landslide toes. In a few other parts of the landslide, particularly along the east flank of the landslide near the toe, displacement vectors are oblique to the displacement contours. These areas are characterized by shearing in addition to shortening.

The changes in displacement can be used to compute average one-dimensional strain at the landslide surface. The extensional strain in the upper part of the landslide increases from about 2 percent near the uppermost cracks to about 20 percent in the region of extensive normal faulting (fig. 1) between the 21- and 24-m displacement contours. Near the toe, the compressional strains range up to about 33 percent while farther upslope, near the 24-m displacement contour, compressional strains are about 4 percent. A neutral zone occurs between the 24-m contours (fig. 3) where strains change from extensional to compressional.

DISCUSSION

Careful mapping of positions and kinds (tension, compression, shear) of features on moving landslides leads to identification of different elements within a landslide and accurate depiction of landslide boundaries. When deformational features are combined with spatial data on displacement, the distribution of deformation can be related to strain on the surface of the landslide. The pattern of deformation on the Twin Lake landslide is large extensional strain in the upper part and large compressive strain at the toe. The neutral area, where the type of deformation changes from stretching to shortening, may separate driving from resisting parts of the landslide. The area of shortening generally resists sliding movement while areas characterized by stretching or nondeformation are the driving elements of the landslide (Baum and Fleming, in review). These deformational data, combined with subsurface information on geometry and pore pressures, can lead to different strategies for remedial treatment depending on the size and geometry of the driving and resisting elements of the landslide.

REFERENCES

Baum, R.L., and Fleming, R.W., in review, Longitudinal forces in landslides--A comparison between field observations and a one-dimensional model: Submitted to Geological Society of America Bulletin, 35 p.

Baum, R.L., Fleming, R.W., and Ellen, S.D., 1989, Maps showing landslide features and related ground deformation in the Woodlawn area of the Manoa Valley, City and County of Honolulu, Hawaii: U.S. Geological Survey Open-File Report 89-290, 2 plates, scale 1:1,200, 16 p.

Baum, R.L., Johnson, A.M., and Fleming, R.W., 1988, Measurement of slope deformation using quadrilaterals, Chapter B in Landslide Processes in Utah--Observation and Theory: U.S. Geological Survey Bulletin 1841, 23 p.

Fleming, R.W., and Johnson, A.M., 1989, Structures associated with strike-slip faults that bound landslide elements: Engineering Geology, v. 27, p. 39-114.

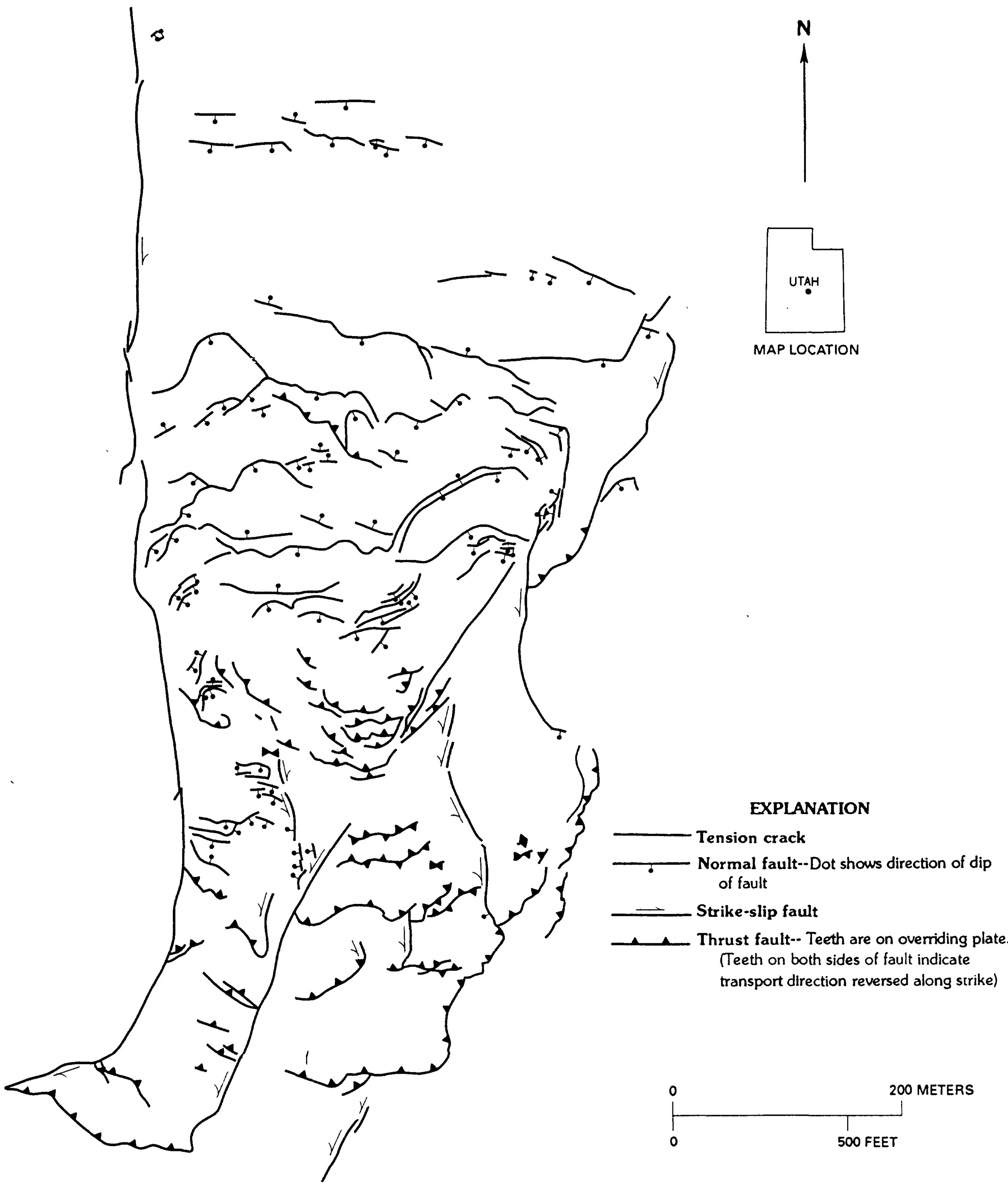

Figure 1. Map showing the pattern of deformation on the surface of the Twin Lake landslide. In general, the deformation is stretching in the upper part and shortening or compression in the lower part of the landslide.

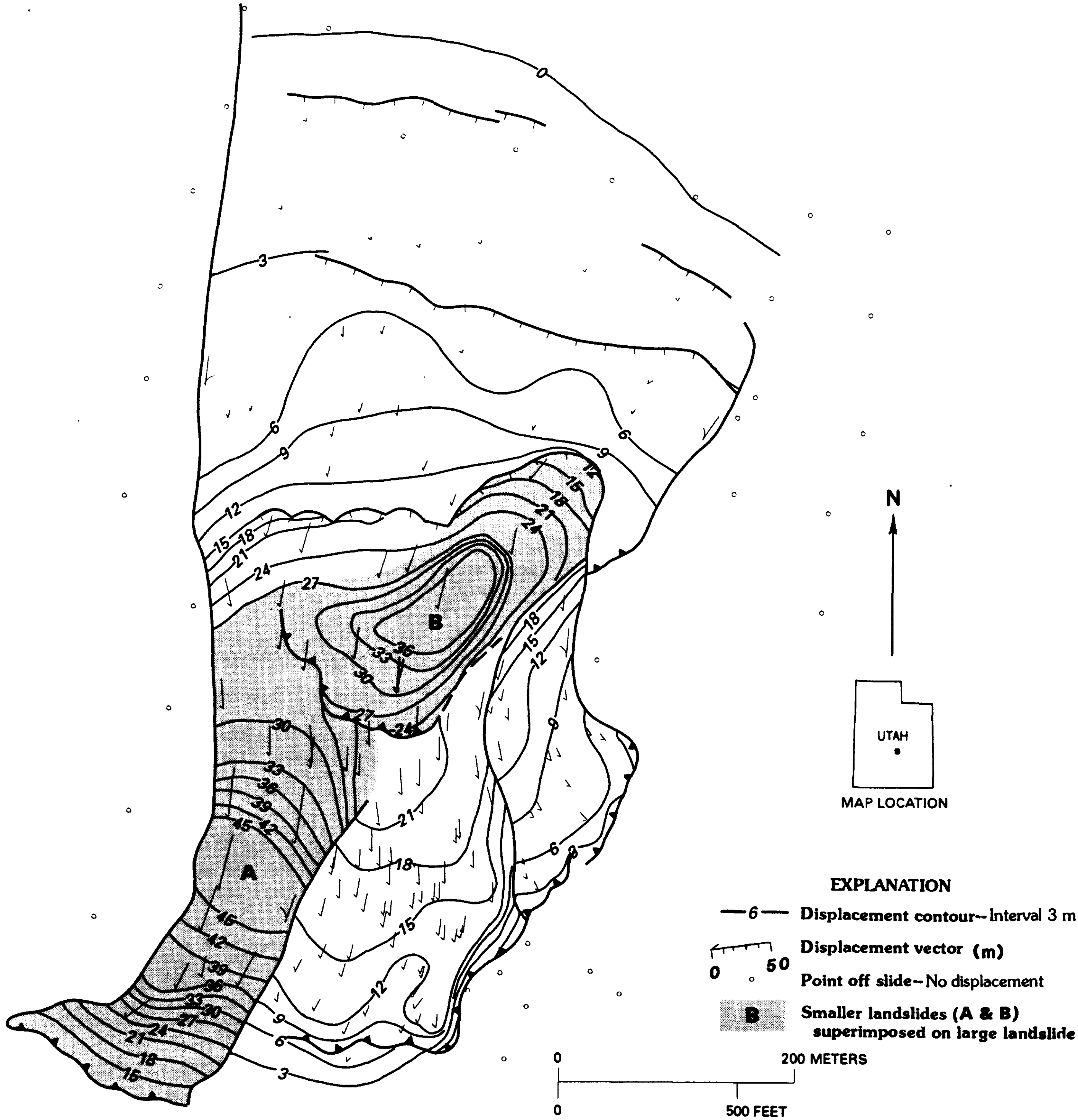

Figure 2. Contours of displacement and displacement vectors on the Twin Lake landslide. Displacement measured from aerial photographs.

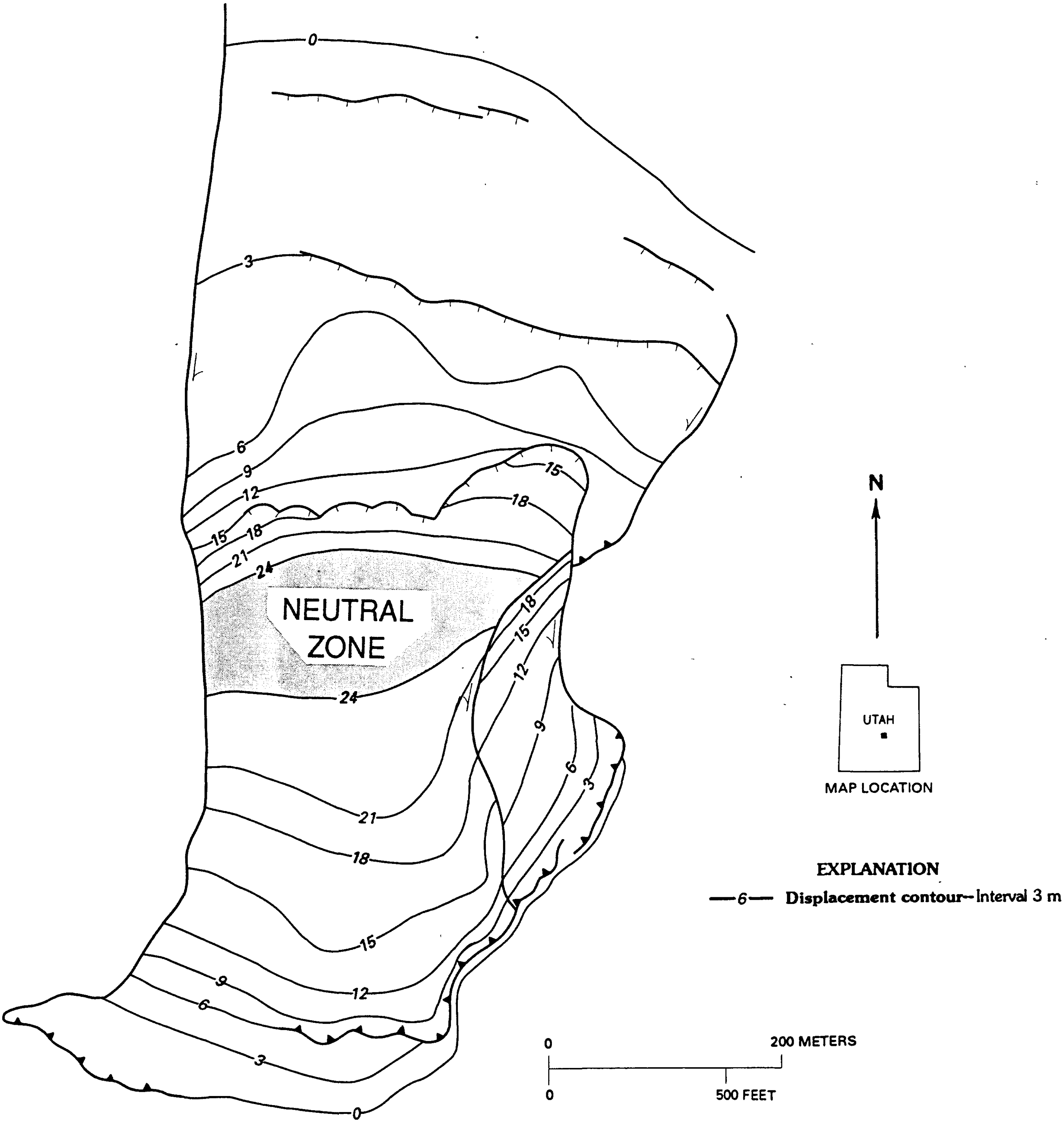

Figure 3. Simplified displacement contours determined by removing the displacement of the superimposed landslides shown on Fig. 2. Shaded area is the general position of the Neutral Zone of the main body of the landslide.